GA–A26241

EXPERIMENTAL STUDY OF FAST WAVE ABSORPTION MECHANISMS IN DIII-D IN THE PRESENCE OF ENERGETIC IONS

by
R.I. PINSKER, M. PORKOLAB, W.W. HEIDBRINK, Y. LUO, C.C. PETTY, R. PRATER, M. CHOI, F.W. BAITY, J.C. HOSEA, R.W. HARVEY, A.P. SMIRNOV, E.F. JAEGER, and M. MURAKAMI

SEPTEMBER 2008

GENERAL ATOMICS

DISCLAIMER

GA–A26241

EXPERIMENTAL STUDY OF FAST WAVE ABSORPTION MECHANISMS IN DIII-D IN THE PRESENCE OF ENERGETIC IONS

by

R.I. PINSKER, M. PORKOLAB,* W.W. HEIDBRINK,† Y. LUO,† C.C. PETTY, R. PRATER, M. CHOI, F.W. BAITY,‡ J.C. HOSEA,§ R.W. HARVEY,¶ A.P. SMIRNOV,¶ E.F. JAEGER,‡ and M. MURAKAMI‡

This is a preprint of a paper to be presented at the 22nd IAEA Fusion Energy Conference, October 13-18, 2008, in Geneva, Switzerland, and to be published in the *Proceedings.*

*Massachusetts Institute of Technology, Cambridge, Massachusetts.
†University of California-Irvine, Irvine, California.
‡Oak Ridge National Laboratory, Oak Ridge, Tennessee.
§Princeton Plasma Physics Laboratory, Princeton, New Jersey.
¶CompX, Del Mar, California.

Work supported in part by
the U.S. Department of Energy
under DE-FC02-04ER54698, SC-G903402, DE-AC05-00OR22725,
DE-AC02-76CH03073, and DE-FG03-99ER54541

GENERAL ATOMICS PROJECT 30200
SEPTEMBER 2008

Experimental Study of Fast Wave Absorption Mechanisms in DIII-D in the Presence of Energetic Ions

R.I. Pinsker 1), M. Porkolab 2), W.W. Heidbrink 3), Y. Luo 3), C.C. Petty 1), R. Prater 1), M. Choi 1), F.W. Baity 4), J.C. Hosea 5), R.W. Harvey 6), A.P. Smirnov 6), E.F. Jaeger 4), and M. Murakami 4)

1) General Atomics, P.O. Box 85608, San Diego, California 92186-5608, USA
2) Massachusetts Institute of Technology, Cambridge, Massachusetts, USA
3) University of California-Irvine, Irvine, California, USA
4) Oak Ridge National Laboratory, Oak Ridge, Tennessee, USA
5) Princeton Plasma Physics Laboratory, Princeton, New Jersey, USA
6) CompX, Del Mar, California, USA

e-mail contact of main author: pinsker@fusion.gat.com

Abstract. DIII-D experiments have studied interaction between injected 80 keV deuterons and fast waves (FWs) at 60 MHz (up to 1.4 MW), 90 MHz (up to 2 MW), and at 116 MHz (up to 1.6 MW), at ion cyclotron harmonic numbers between 4 and 8. While strong absorption of FWs at the 4th harmonic of injected deuterons has been clearly observed, ion absorption under the same conditions at 6th and 8th harmonics is seen to be weak. Data on fast wave absorption on the injected beam is obtained from confinement analysis and equilibrium reconstruction, from fusion neutron rate measurements, and from fast ion D_α (FIDA) spectroscopy. Strong acceleration of the beam above the injected energy in the 4th harmonic case, weak acceleration in some of the 6th harmonic cases, and no acceleration in the 8th harmonic cases is observed with the FIDA diagnostic. The experimental results also indicate clearly the importance of edge losses in cases in which the central absorption mechanisms are weak. Therefore quantitative modeling must take the edge losses into account. Core absorption mechanisms will be much stronger in ITER, so that edge losses should be much less significant than in DIII-D, but the competition between core damping mechanisms will be similar. Hence, establishment of a quantitative model of the partitioning of FW power among competing absorption processes is important in both cases.

1. Introduction

Experiments on DIII-D have shown that fast Alfvén waves (FWs) can be damped on core electrons with minimal damping on fast ions at high harmonics [1], despite the possibility of strong fast ion absorption. Fast wave current drive (FWCD) is an option for central current drive in ITER, especially in view of the difficulty of achieving sufficiently high energy and power in negative-ion-based neutral beams for this application. Since ITER and any future fusion reactor will necessarily have large fast ion populations (alphas and perhaps injected ion species), it is important to have a validated quantitative model of the interaction between fast ions and FWs to assess the application of FWs for central heating and current drive. For FWCD, in which the intended absorption mechanism is Landau damping on electrons [2–4], absorption by ion cyclotron harmonic damping would reduce the available power to the electrons for heating and current drive. These DIII-D experiments have studied interaction between injected 80 keV deuterons and FWs at 60 MHz, 90 MHz, and at 116 MHz, at ion cyclotron harmonic numbers between 4 and 8. (Previous DIII-D work in this area studied absorption of 60 MHz and 83 MHz FWs on injected beam ions [5-7].)

The outline of this paper is as follows. First, the experimental data comparing absorption of FWs at the 4th, 6th, and 8th harmonics at a constant toroidal field of about 2 T are presented. Since an initially thermal hydrogen minority, present in all nominally deuterium plasmas at some low level (typically <1% in DIII-D), could absorb power at half the harmonic number of the deuterium (for even-numbered harmonics), the hydrogenic species mix was increased at the same 2 T field, and the results compared with those from nominally pure deuterium plasmas. The two important dimensionless parameters for ion cyclotron harmonic damping of FWs at an angular frequency ω on an ion species with characteristic speed perpendicular to the field lines $v_\perp$ are ω/Ω_i and $v_\perp/v_A$ where v_A is the Alfven velocity and Ω_i is the angular ion cyclotron frequency. Changing the harmonic number at fixed plasma parameters by changing the FW frequency changes only the first parameter, while varying the toroidal field at fixed frequency necessarily changes both dimensionless parameters. Such a toroidal field scan was carried out at a fixed FW frequency of 60 MHz with other parameters held as constant as practical, covering the range of deuterium harmonics from 4th to 7th. Finally, results from a recent experiment are shown in which absorption of 60 MHz FWs at the 4th harmonic accelerates injected deuterons to provide a target for 90 MHz FWs (6th harmonic). Comparison of the effect of 60 MHz and 90 MHz alone to the effect of the combined power provides evidence of “synergy”: that is, the effect of the two harmonics separately summed together is smaller than the effect of the combined power. A discussion of these results concludes the paper, in which several kinds of theoretical models are used to explain the results. The effect of edge losses, which have been previously shown to be important in DIII-D FWCD experiments, is considered

2. Comparisons of 2nd, 4th, 6th and 8th Harmonic Absorption at Fixed Toroidal Field

While strong absorption of FWs at the 4th harmonic on injected deuterons has been clearly observed, ion absorption under the same conditions at 6th and 8th harmonics is generally weak. An experiment was performed in which 1.66 MW of FW power at 116 MHz (8th harmonic near the magnetic axis at toroidal field B_T = 1.85 T) was coupled to an L-mode discharge with 5 MW of 80 keV deuterium neutral beam injection; later in the same discharge, the effect of 1.1 MW of FW power at 60 MHz (4th harmonic just inboard of the magnetic axis) was compared with that of the 8th harmonic power. The effect of the FW was isolated by comparing this discharge with an otherwise identical discharge with no FW power. These comparisons are shown in Fig. 1, where differences in the plasma stored energy and in fusion neutron rate between the discharges with and without FW power are shaded. It is evident from the fusion neutron rate that the acceleration of beam ions by the FW is much stronger for the 4th harmonic case than for the 8th, though the coupled 8th harmonic power is 50% higher than the 4th harmonic power.

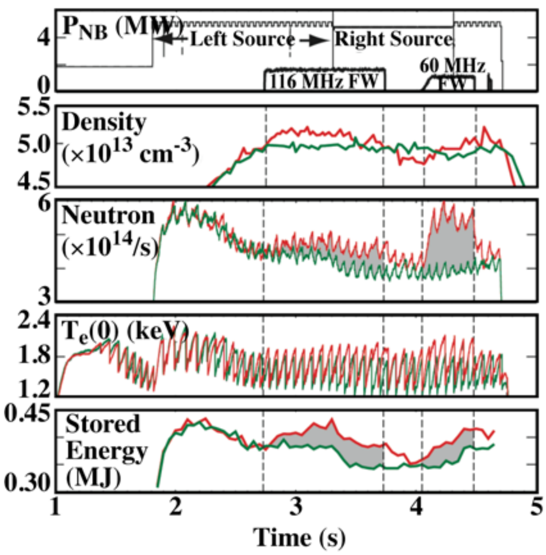

FIG. 1. Time history of high density L-mode discharge comparing 4th (60 MHz) and 8th harmonic (116 MHz) FW heating at 1.85 T, I_p =1.2 MA. Dotted vertical lines show rf on and off times. Green traces from comparison case with no FW.

In these experiments, the FW/fast ion interaction was measured directly using the fast ion D_α (FIDA) spectroscopy diagnostic technique [8], which involves vertically-viewed D_α charge exchange recombination emission from one of the injected beams. This diagnostic confirmed that the absorption of the FW power at the 4th harmonic accelerates deuterons near the injection energy of 80 keV, with a 65% enhancement of the signal in the 60–80 keV range, as well as accelerating particles to higher energy than the injection energy. The density of accelerated ions observed with this instrument is correlated with the enhanced fusion neutron emission rate. FIDA confirmed that the interaction at the 8th harmonic is much weaker than at the 4th (with identical plasma density, magnetic field, beam energy and power).

Sixth harmonic absorption on fast ions is also weak by comparison with that at the 4th harmonic at the same toroidal field. Experiments compared 6th harmonic absorption of up to 2 MW of 90 MHz FW power with 4th harmonic absorption of 60 MHz FWs. At the lowest plasma density studied, the FIDA diagnostic observed weak beam acceleration in the 6th harmonic case at 2 T compared with that observed in the 4th harmonic case. At higher density, no beam acceleration was observed in the 6th harmonic case and only electron damping was found. Using an offset linear confinement model [9] to characterize the incremental effect of the FW power on the beam-heated target plasma, we compare the incremental confinement time $\tau_{inc} \equiv \Delta W / P_{FW}$, where ΔW denotes the increase in stored energy caused by the FW power, to the global confinement time $\tau_0 \equiv W / (P_{NBI} + P_{OH})$ in the target. We find that the ratio $\tau_{inc}/\tau_0 = 0.5$ for the lower density 6th harmonic case ($\bar{n}_e = 2 \times 10^{19}$ m^{-3}, P_{NBI} = 1.4 MW, P_{FW} = 0.9 MW), while $\tau_{inc}/\tau_0 = 0.24$ for the higher density case ($\bar{n}_e = 3.5 \times 10^{19}$ m^{-3}, P_{NBI} = 1.4 MW, P_{FW} = 1.2 MW). Applying the same analysis to a similar low density discharge that had 60 MHz FW (4th harmonic), we find $\tau_{inc}/\tau_0 = 1.0$, i.e., no apparent confinement degradation ($\bar{n}_e = 2 \times 10^{19}$ m^{-3}, P_{NBI} = 2.4 MW, P_{FW} = 0.9 MW). The interpretation of these confinement results is that in the 4th harmonic case, the substantial acceleration of the injected fast ions produces a plasma dominated by fast ions and has the improved confinement characteristic of such discharges with reduced ion/electron coupling; the 6th harmonic low density case has much lower incremental fast ion content due to the reduction in absorption going from 4th to 6th harmonic, so the confinement shows a typical degradation with incremental power, while in the higher density 6th harmonic case, the fast ion content in the target, 6th harmonic damping on the fast ions, and the direct electron damping are all strongly reduced. The reduction in the direct electron damping of the FWs in the 6th harmonic case in the higher density case is due to the lower electron temperature compared with the lower density. Thus increasing the density reduces the single-pass absorption from both direct electron damping and by 6th harmonic absorption on the fast ions. The apparent poor incremental confinement in this case is explained as a reduction in the fraction of the coupled power that is absorbed in the core. As previously had been established in DIII-D FWCD experiments [10], in L-mode plasmas similar to these an edge loss of about 4% per bounce competes with the core absorption, so if the total single-pass damping (the sum of the direct electron damping and the ion cyclotron harmonic damping) were of the same order per pass through the core, the fraction of the coupled power that is absorbed in the core would be significantly reduced. These results on incremental confinement are shown in Table I.

TABLE I. Incremental confinement fraction results at 2 T for harmonics from 2nd to 8th with deuterium neutral beam preheating. Counter-current phasing in all cases, I_p =1–1.2 MA.

$\bar{n}_e$ (10^{19} m^{-3})	FW Freq. (MHz)	Harmonic	P_{FW} (MW)	$P_{NBI} + P_{OH}$ (MW)	τ_{inc}/τ_0
5	116	8	1.66	5.5	0.24 ±0.06
3.5	90	6	1.2	1.4	0.24
2	90	6	0.9	1.4	0.5
5	60	4	1.1	5.5	0.45
2	60	4	0.9	2.4	1.0
3	60	4	1.1	2.7	1.0 (before s/t crash) 0.75 (after s/t crash)
2.5	60	2 (H/[H+D]=0.25)	0.9	4.2	1.0

3. Effect of Significant Hydrogen Minority on 60 MHz FW Absorption at 2 T

Competition between absorption on fast deuterons and on (initially) thermal protons at half the harmonic number was studied in mixed hydrogen/deuterium plasmas with deuterium beam injection. The hydrogen fraction was $H/(H+D) = 0.25 \pm 0.05$, measured by the usual H_α / D_α spectroscopic technique. Almost no neutron enhancement was observed upon injection of 0.9 MW of 60 MHz FW into a 1 MA discharge at 1.95 T with 3.8 MW deuterium beam power. The difference between the diamagnetic measurement of stored energy and the measurement based on MHD equilibrium increases during FW injection, indicating increased perpendicular energy in the fast protons. The ratio of the incremental confinement time to the global confinement in the beam injected target was $\tau_{inc}/\tau_0 = 1.0$ (see the last entry in Table I). As in the best 4th harmonic deuterium case, the enhanced fast ion (proton) content in the plasma yields improved confinement. A significant difference between the 2nd harmonic hydrogen and 4th harmonic deuterium cases is that no tendency towards sawtooth stabilization has yet been observed in the hydrogen cases, in contrast to the partially stabilized sawteeth often obtained in the DIII-D 4th harmonic cases [7]. (The effect of the higher fast ion content in the partially stabilized sawtooth case is displayed in the sixth entry in Table I – a 23% drop in incremental confinement occurs after the first sawtooth crash.) In discharges subsequent to the $H/(H+D)=0.25$ case discussed here, high power deuterium beam heating progressively lowered the hydrogen fraction to the usual level of $H/(H+D)=0.01\pm 0.01$ over the course of about 25 tokamak discharges, and the neutron enhancement, partial sawtooth stabilization and other signatures of the pure deuterium 4th harmonic absorption returned to the same levels as prior to the introduction of hydrogen.

4. Variation of Harmonic Number at Fixed FW Frequency

In the results discussed to this point, the harmonic number was varied by changing the FW frequency (Sec. 2) or the ion species (Sec. 3) at fixed toroidal field. The other possibility is to vary the toroidal field at fixed FW frequency and ion species. In the high harmonic limit the maximum interaction between an energetic ion with perpendicular velocity $v_\perp$ and the FW occurs for $v_\perp$ near the the Alfven velocity v_A. The Alfven velocity is proportional to the magnetic field strength, so when the absorption is on sub-Alfvenic injected beam ions of a fixed energy, the absorption increases as the toroidal field is reduced, i.e. as the harmonic number increases at a fixed FW frequency. Previously reported DIII-D FW experiments [5,6] have analyzed fast ion absorption as a function of toroidal field at fixed FW frequency, but those results were complicated by the simultaneous use of two FW frequencies (60 and 83 MHz). In the present work, a similar downwards toroidal field scan is carried out using FWs at 60 MHz alone. A maximum in absorption on the injected deuterium beams was found as the fifth harmonic of deuterium passed through the magnetic axis. Strong deuterium acceleration was observed both from the FIDA diagnostic and from the fusion neutrons [1,8]. Another significant aspect of strong neutron enhancement in the fifth-harmonic discharge is that absorption on a small (<1%) residual (thermal) hydrogen fraction is minimized in that odd-numbered deuterium cyclotron harmonic case, since no hydrogen harmonic is present near the axis. In this fifth harmonic discharge, the spatial profile of the fast ion interaction was measured with FIDA [8]; the observed peak of the acceleration occurs at a slightly larger major radius than the major radius at which $\omega = 5\Omega_D$.

The L- to H-mode transition threshold power scales approximately linearly with toroidal field. To keep the discharge in L-mode (to retain density control and thereby maintain a high fast ion content), the neutral beam power was reduced as the field was lowered. The beam power was controlled at fixed beam energy by pulse-modulating the beam at a frequency much higher than the inverse of the fast ion slowing-down time, lowering the duty factor at lower fields. The lowest field at which these data have been obtained so far is 1.2 T, at which the 6th deuterium harmonic for 60 MHz is 15 cm inboard of the magnetic axis and the 7th harmonic is 11 cm outboard of the magnetic axis. In this case, the average neutral beam power is 0.5 MW, while the 60 MHz FW power is 1.1 MW. The pulses in the fusion neutron rate (almost entirely beam-target reactions under these conditions) were analyzed using the technique described in Ref. [11], with the results shown in Fig. 2. The analysis clearly shows that the beam ions are accelerated by the high harmonic interaction. Both the time-averaged level of neutron emission and the decay time constant of the pulses increase substantially upon injection of FW power. The decay time constant before the FW is 11.0±0.2 ms, while after a steady-state is reached during the FW, the time constant is 39.0±2.0 ms, while the average level of the neutron emission rises by about a factor of three. The reason that the decay time constant increases during the FW is that the size of the tail of the distribution is determined by a competition between Coulomb drag and acceleration by cyclotron absorption; the high-energy ions that dominate the D-D beam-target fusion neutron rate experience strong acceleration that, on average, nearly arrests Coulomb drag. TRANSP [12] analysis using measured temperature, density, impurity and rotation profiles (but not including any model for FW-induced acceleration) shows that this increase in neutron emission is not due to electron heating increasing the fast ion density by increasing the

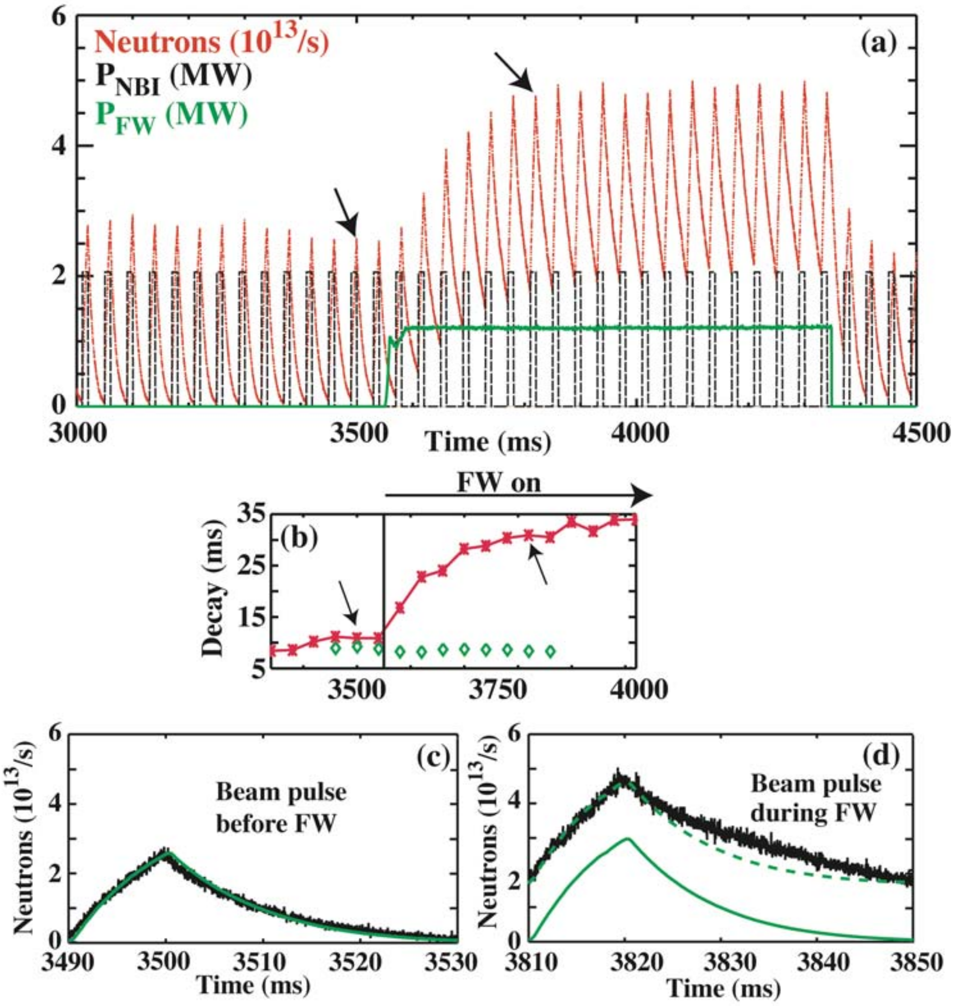

FIG. 2. Damping of FW power at 6th and 7th harmonics on an injected beam. (Deuterium, 60 MHz FW, toroidal field at the center is 1.2 T [ω/Ω_D = 6.4 at the magnetic axis], line-averaged density is 3×10^{19} m^{-3}, plasma current is 0.6 MA.) (a) 80 keV D beam power (dashed black), 60 MHz FW power (solid green), and neutron rate (dotted red) time histories. (b) Decay time constant of neutron rate pulses calculated by TRANSP with the measured profiles but not taking into account FW-induced acceleration of beam ions (open green diamonds) just before and during the first 0.3 s of the FW pulse, compared with the best-fitting decay times from each measured neutron pulse (red asterisks and connecting line). (c) Detail of measured neutron pulse just before the FW [indicated with an arrow on (a) and (b)] and TRANSP prediction (solid green curve). (d) Detail of measured neutron pulse during the FW pulse [indicated with an arrow on (a) and (b)] and TRANSP prediction not including FW acceleration (solid green curve). The TRANSP prediction is also shown translated upwards (dashed green curve) to facilitate comparison of the curvatures of the predicted and measured neutron rates.

slowing-down time. The predicted decay rates are in good agreement with the measured values before the FW injection, but the predicted decay rate drops slightly upon injection of the FW, due to the density rise engendered by the FW. The density increase is predicted to have a stronger effect on the slowing-down time than the slight increase in the average electron temperature. The detailed comparison of the model to the experimental neutron rate is shown for a typical neutron pulse before the FW (part [c] of the figure) and during the FW [Fig. 2(d)]. The risetime of the neutron pulses is accurately modeled by TRANSP both before and during the FW, because the beam ions that have just been injected have not had time to be accelerated, so they produce the same number of neutrons before and during the FW. The characteristic time to accelerate the ions is evident from the timescale on which the decay time increases, shown in Fig. 2(b).

In a similar discharge, FIDA data also showed evidence of beam acceleration above the injection energy at this 6th/7th harmonic condition at 1.2 T.

5. Synergy Between 4th and 6th Harmonic Absorption on Fast Ions at 2 T

Since at a fixed value of toroidal field the interaction between the FW and fast ions maximizes at higher energies as the harmonic number increases, the high harmonic damping should be substantially increased with an increase in the maximum ion energy in the injected beam. Either increasing the beam acceleration voltage or rf acceleration of the injected beam ions in the plasma with a lower harmonic FW should have a similar effect. This hypothesis was tested by comparing the effect of 60 MHz FWs (4th harmonic), 90 MHz FWs (6th harmonic), and the simultaneous application of 60 and 90 MHz power to a 2 T beam-heated discharge. The effects of separate 60 MHz (1.1 MW) and 90 MHz (1.5 MW) pulses are shown in Fig. 3(a), where the measured neutron rate is compared with the TRANSP prediction using measured profiles but not taking into account FW acceleration. 60 MHz produces a typical clear neutron enhancement while the higher power 6th harmonic FW produces only a very small increase in neutron rate beyond the TRANSP prediction. FIDA also shows evidence of acceleration above the beam injection energy for both the 4th and 6th harmonic FW, though the signals were not as clear as in most other cases for reasons that are

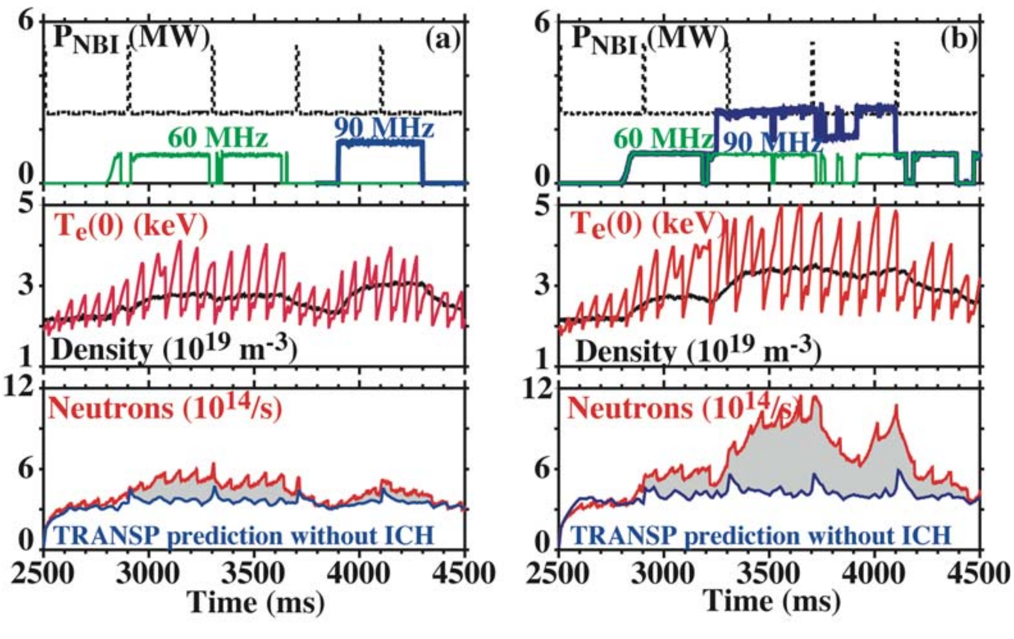

FIG. 3. Comparison of (a) the separate effects of 4th and 6th harmonic absorption in a 2 T, 1.2 MA discharge with (b) their combined effect, showing a strong synergy in the neutron signal.

not yet understood. The ratio of τ_{inc}/τ_0 is 0.85 and 0.59 for 60 and 90 MHz, respectively, showing the improvement in global confinement with enhanced fast ion content as before.

Next, the 6th harmonic power (1.6 MW) was overlapped with the 4th harmonic power (1.1 MW). The 60 MHz power was allowed to accelerate the beam ions for 0.45 s before the addition of the 90 MHz FW, which both the previous experimental results and time-dependent modeling of the tail formation [6] showed is needed for the tail to develop fully. The added 90 MHz power nearly triples the enhancement in the neutron rate above the TRANSP no-acceleration prediction. The effect of the 90 MHz combined with 60 MHz pre-acceleration on the neutron rate is much larger than the sum of their individual effects, i.e., a "synergy" is obtained. The global confinement shows at most only a weak synergistic effect – the incremental confinement of the combined 60 and 90 MHz heating is only slightly higher than the power-weighted average of the incremental confinement values for the separate 60 and 90 MHz heating cases. A much stronger synergy in the neutron rate than in the global confinement is expected, because the D-D fusion cross-section increases strongly with ion energy and is therefore weights the highest energy part of the fast ion distribution much more strongly than the stored energy. As pointed out in [6], only a small fraction of the coupled FW power is needed to account for the increase in neutron rate, while the stored energy increase is due to the total of the power damped on fast ions and the power directly damped on electrons.

6. Discussion

The total single-pass core absorption in the cases studied experimentally in this work is the sum of the ion cyclotron harmonic damping on thermal and non-thermal (injected species and FW-accelerated ions) ion species and the direct electron damping via the coherent combination of electron Landau damping and the TTMP interaction [2,3]. At the plasma edge region another set of wave damping mechanisms can be of importance, including rectified rf sheaths at the wall, parametric decay and subsequent absorption of daughter waves, collisional damping, etc. These edge dissipation mechanisms have been discussed from both experimental [13] and theoretical viewpoints [14]. Under conditions in which the core damping is weak (fraction of the power absorbed in a single pass through the core $\eta_{core} << 1$), which is typical of the L-mode plasmas studied in this work and relatively low neutral beam power levels, then the waves make multiple passes through the core and edge regions. If the edge absorption mechanisms are weak (the usual case), the fraction of the wave power lost per transit of the edge region $\eta_{edge} << 1$. After multiple passes of the power through the core and edge regions, then, the fraction of the coupled FW power absorbed in the core is $\langle\eta_{core}\rangle / \left(\langle\eta_{core}\rangle + \langle\eta_{edge}\rangle\right)$ in which the absorbed fractions are averaged over many passes. A similar partitioning of power among competing damping mechanisms occurs in the core region, in these cases between the direct electron damping and the ion cyclotron harmonic absorption. Again the partitioning is determined by the relative strength of the competing damping mechanisms.

Previous DIII-D work on FWCD in which the dominant core power absorption mechanism is direct electron damping has shown that an edge loss at the level of a few percent per bounce is needed to quantitatively account for the observed current drive efficiency in L-mode discharges, in which the denominator in the current drive efficiency was taken to be the net power coupled from the antenna [10]. Under similar edge plasma conditions, similar levels of edge losses will play a role in determining the partition between edge and core absorption as long as the sum of all core damping mechanisms $\eta_{core} << 1$.

It is therefore not surprising that large-scale simulations that do not include edge losses do not fully agree with the results from these experiments in the low single-pass absorption regime. These experiments have been modeled with the combination [15] of the AORSA full-wave code and the CQL3D bounce-averaged Fokker-Planck code, CQL3D combined with the GENRAY ray-tracing model, and the ORBIT-RF Monte Carlo code combined [16] with the TORIC full-wave model. So far these models are not fully in agreement with each other; rough agreement with the experimental results is obtained in some cases. In cases where the edge losses per bounce and the core absorption per transit are comparable, the level of edge losses will strongly affect the FW amplitude in the core of the plasma. Since that FW amplitude is crucial in a quasi-linear model, efforts are ongoing to assess the importance of various edge loss mechanisms in resolving the remaining discrepancies between the predictions of the models and the experimental results. Modeling the competition between direct electron absorption in the core, fast ion absorption in the core and edge losses is simpler in a ray-tracing approach, so the CQL3D/GENRAY approach is being used to study the partitioning of wave energy between these absorption channels. Incorporation of an edge loss model in the full-wave approach is ongoing; a related wave-kinetic approach appropriate to the weak single-pass damping regime was developed in Ref. [17], where a simple model for unspecified losses was included.

The single-pass absorption will be much stronger in ITER, so that edge losses should be much less significant than in DIII-D (though possibly still significant from the point of view of ICRF-specific impurity production in a high-Z environment), but the competition between core damping mechanisms will be in some ways qualitatively similar to the situation in DIII-D, since ITER will have high densities of energetic ions from alphas and injected beams. Since the fast ion distribution functions of ions from neutral beam injection at the MeV energy scale and of fusion alphas will be different from the distribution resulting from 80 keV deuterium beam injection in DIII-D, the expected FW damping at cyclotron harmonics on ITER will be quantitatively different from damping on DIII-D. But to enable the calculation of partitioning of FW power among the competing absorption processes for ITER, the establishment of a quantitative, experimentally benchmarked model on DIII-D will be an important step.

Acknowledgments

This work was supported by the US Department of Energy under DE-FC02-04ER54698, SC-G903402, DE-AC05-00OR22725, DE-AC02-76CH03073, and DE-FG03-99ER54541.

References

[1] PINSKER, R.I., *et al.,* Nucl. Fusion **46**, S416 (2006).
[2] STIX, T.H., Nucl. Fusion **15**, 737 (1975).
[3] PORKOLAB, M., in *Thomas H. Stix Symp. On Advances in Plasma Physics* (Princeton, NJ, 4-5 May 1992) (New York, AIP, 1994) 99.
[4] CHIU, S.C., *et al.,* Nucl. Fusion **29**, 2175 (1989).
[5] PETTY, C.C., *et al., Proc. 12th Top. Conf. on Radio Frequency Power in Plasmas* (Savannah, Georgia, 1997) (New York, AIP, 1997) 225.
[6] MANTSINEN, M.J., *et al.,* Phys. Plasmas **9**, 1318 (2002).
[7] HEIDBRINK, W.W., et al., Nucl. Fusion **39**, 1369 (1999).
[8] HEIDBRINK, W.W., *et al.*, Plasma Phys. Control. Fusion **49**, 1457 (2007).
[9] BHATNAGAR, V.P., *et al.,* Plasma Phys. Control. Fusion **31**, 333 (1989).
[10] PETTY, C.C., *et al.,* Nucl. Fusion **35**, 773 (1995).
[11] HEIDBRINK, W.W., et al., Nucl. Fusion **43**, 883 (2003).
[12] http://w3.pppl.gov/transp
[13] NOTERDAEME, J.-M. and VAN OOST, G., Plasma Phys. Control. Fusion **35**, 1481 (1993).
[14] MYRA, J.R., *et al.,* Nucl. Fusion **46**, S455 (2006).
[15] JAEGER, E.F., *et al.,* in *Proc. 17th Top. Conf. on Radio Frequency Power in Plasmas* (Clearwater, Florida, 2007) (New York, AIP, 2007) 443.
[16] CHOI, M., *et al.,* Nucl. Fusion **46**, S409 (2006).
[17] KUPFER, K., *et al.,* Phys. Plasmas **1**, 3915 (1994).